Redox Biology 66 (2023) 102863

Contents lists available at ScienceDirect

Redox Biology

journal homepage: www.elsevier.com/locate/redox

Low-dose LPS alleviates early brain injury after SAH by modulating microglial M1/M2 polarization via USP19/FOXO1/IL-10/IL-10R1 signaling

Weihua Tao [a,1], Guibo Zhang [a,1], Chengyuan Liu [a], Lide Jin [a], Xuehua Li [b,**], Shuaifeng Yang [a,*]

[a] Department of Neurosurgery, The First People's Hospital of Yunnan Province/The Affiliated Hospital of Kunming University of Science and Technology, China
[b] Center for AIDS/STD Control and Prevention, Yunnan Center for Disease Control and Prevention, Kunming, Yunnan, China

ARTICLE INFO

Keywords:
Lipopolysaccharide
Subarachnoid hemorrhage
USP19
FOXO1
IL-10

ABSTRACT

Background: Low-dose lipopolysaccharide (LPS) protects against early brain injury (EBI) after subarachnoid hemorrhage (SAH). However, the mechanism underlying the neuroprotective roles of low-dose LPS remain largely undefined.

Methods: A SAH mice model was established and the pathological changes of brain were evaluated by wet-dry weight method, HE and Nissl staining, and blood-brain barrier (BBB) permeability assay. Cell apoptosis and inflammation were monitored by TUNEL, flow cytometry and ELISA assays. qRT-PCR, immunofluorescence and Western blot were used to detect the expression of microglial polarization-related or oxidative stress-associated markers. Bioinformatics analysis, luciferase and ChIP assays were employed to detect the direct association between FOXO1 and IL-10 promoter. The ubiquitination of FOXO1 in the *in vitro* SAH model was detected by co-IP.

Results: Low-dose LPS alleviated SAH-induced neurological dysfunction, brain edema, BBB disruption, damage in the hippocampus, neuronal apoptosis and inflammation via modulating microglial M1/M2 polarization by IL-10/IL-10R1 signaling. Mechanistic studies showed that FOXO1 acted as a transcriptional activator of IL-10. USP19 mediated the deubiquitination of FOXO1 to activate IL-10/IL-10R1 signaling, thereby regulating microglial M1/M2 polarization. Functional experiments revealed that low-dose LPS upregulated USP19 to modulate microglial M1/M2 polarization via FOXO1/IL-10/IL-10R1 signaling in SAH mice.

Conclusion: Low-dose LPS protected against EBI after SAH by modulating microglial M1/M2 polarization via USP19/FOXO1/IL-10/IL-10R1 signaling.

1. Introduction

Subarachnoid hemorrhage (SAH) is a cerebrovascular disease with high mortality worldwide [1]. Early brain injury (EBI), including neuroinflammation, brain edema, blood-brain barrier (BBB) disruption, increased intracranial pressure (ICP) and neuronal apoptosis, has been considered as a key contributor to unfavorite prognosis of patients with SAH [2,3]. The brain-resident microglia and microglia-driven neuroinflammation are emerging as crucial players in SAH. Microglia accumulation or activation is observed after SAH [4,5]. Previous studies have demonstrated the neuroprotective role of low-dose lipopolysaccharide (LPS) after SAH [6,7]. More importantly, LPS preconditioning leads to decreased accumulation and activation of microglia following SAH [8]. However, detailed mechanism underlying the neuroprotective effects of LPS after SAH remains largely undefined.

Ubiquitination is implicated in a variety of biological processes in eukaryotic cells [9]. Ubiquitin-activating enzyme E1, ubiquitin-conjugating enzyme E2 and ubiquitin ligase E3 work in concert to conjugate ubiquitin to a substrate protein [10]. By contrast, deubiquinases (DUBs) remove ubiquitin conjugates from substrates [11]. Ubiquitin-specific protease 19 (USP19), one of the DUBs, localizes in endoplasmic reticulum (ER) and contributes to DNA damage repair and degradation of ER-associated protein [12,13]. Previous studies have demonstrated that USP19 mediates the deubiquination of TAK1 and TRIF, thereby inhibiting TNF-α/IL-1β and TLR3/4 signaling, respectively [14,15]. A more recent study has illustrated that USP19 acts as an anti-inflammatory regulator and facilitates M2 macrophage polarization

* Corresponding author.
** Corresponding author.
E-mail addresses: 13668702530@163.com (X. Li), yangshuaifeng7@163.com (S. Yang).
[1] These authors are co-first authors.

https://doi.org/10.1016/j.redox.2023.102863
Received 16 June 2023; Received in revised form 3 August 2023; Accepted 25 August 2023
Available online 26 August 2023
2213-2317/© 2023 The Authors. Published by Elsevier B.V. This is an open access article under the CC BY-NC-ND license (http://creativecommons.org/licenses/by-nc-nd/4.0/).

Abbreviations

ACA	anterior cerebral artery
ATCC	American Type Culture Collection
BBB	blood-brain barrier
ChIP	chromatin immunoprecipitation
co-IP	co-immunoprecipitation
DUBs	deubiquinases
EB	Evans blue
EBI	early brain injury
ER	endoplasmic reticulum
FOXO1	forkhead box protein O1
Gpx	glutathione peroxidase
HE	Hematoxylin Eosin
ICA	internal carotid artery
ICP	increased intracranial pressure
IF	immunofluorescence
IFN-γ	interferon-γ
IL-10	interleukin-10
LPS	lipopolysaccharide
I/R	ischemia/reperfusion
MCA	middle cerebral artery
OHb	oxyhemoglobin
SAH	subarachnoid hemorrhage
TUNEL	terminal deoxynucleotide transferase-mediated dUTP-biotin nick end labeling
USP19	ubiquitin-specific protease 19

[16]. It is worth noting that USP19 knockout mice exhibit more serious inflammation in response to LPS [15], raising the possibility that USP19 might be involved in mediating the neuroprotective role of LPS after SAH.

Forkhead box protein O1 (FOXO1), a well-studied member of FOX family, acts as a transcription factor to modulate downstream targets involved in cell apoptosis, autophagy, cell cycle arrest, oxidative stress and immune regulation [17]. FOXO1 improves SAH-induced neurological function, brain edema, BBB leakage and inflammation by promoting autophagy in rat [18]. Intriguingly, low-dose LPS protects against ischemia/reperfusion (I/R)-induced neuronal apoptosis by increasing FOXO1 and phosphorylated FOXO1 (p-FOXO1) [19]. Bioinformatic analysis based on Ubibrowser 2.0 predicted that USP19 might mediate the deubiquitination of FOXO1. Whether low-dose LPS regulates FOXO1 expression via USP19-dependent deubiquitination merits in-depth investigation.

In human and mouse, the anti-inflammatory cytokine Interleukin-10 (IL-10) is released by microglia upon interferon-γ (IFN-γ) or LPS treatment [20,21]. Previous study has demonstrated that lack of IL-10 promotes microglial M1 polarization [22]. Our preliminary data showed that IL-10 ameliorated brain edema and neurological function following SAH. The putative binding site between FOXO1 and IL-10 promoter was predicted using JASPAR database. Recent study has reported that FOXO1 binds on the KLF5 promoter and positively regulates its expression in cardiomyocyte, thereby contributing to diabetic cardiomyopathy [23]. It is of interest to investigate if IL-10 functions as a downstream target of FOXO1 in SAH.

To further unravel the mechanism underlying the protective effects of low-dose LPS on EBI after SAH, we hypothesized that low-dose LPS might upregulate USP19 to mediate the deubiquitination of FOXO1, thereby activating IL-10/IL-10R1 signaling to modulate microglial M1/M2 polarization, ultimately ameliorating EBI after SAH. These data will provide novel insight into the targeted therapy of SAH.

2. Materials and methods

2.1. Animal study

Male C57BL/6 mice (10 ~ 12-weeks old) were from Shanghai SLAC Laboratory Animal Co.,Ltd. All animal studies were approved by the Ethics Committee of the Animal Ethics Council of Kunming University of Science and Technology (No. LA2008305). The total animal number, mortality and exclusion rates were included in Fig. S2B. Subarachnoid hemorrhage (SAH) model was established as previously described [24]. Briefly, the right internal carotid artery (ICA) was dissected after anesthetization. The bifurcation of anterior cerebral artery (ACA) and middle cerebral artery (MCA) were punctured through the ICA by using a sharpened nylon. Mice in Sham group underwent same surgery without artery perforation.

Experiment 1 Mice were divided into four groups (n = 5 per group): Sham, SAH, SAH + saline (NaCl) and SAH + LPS (low). LPS preconditioning was conducted as described [7]. In brief, mice were intraperitoneally injected with lipopolysaccharide (LPS, 140 mg/kg, Sigma-Aldrich, St. Louis, MO, USA) or saline 24 h prior to SAH induction. The selection of this dose was based on our preliminary data (Fig. S2C) and previously published report [7]. High dose of LPS (280 mg/kg) induced unacceptable mortality within 24 h (Fig. S2C).

Experiment 2 Mice were divided into five groups (n = 5 per group): Sham, SAH, SAH + LPS, SAH + LPS + sh-NC and SAH + LPS + sh-IL-10. Mice received scrambled shRNA (sh-NC) or sh-IL-10 lentivirus (Sangon Biotech, Shanghai) microinjection as described [25]. After 48 h, mice were treated with LPS, followed by SAH induction.

Experiment 3 Mice were divided into six groups (n = 5 per group): Sham, SAH, SAH + LPS, SAH + LPS + sh-NC + OE-NC, SAH + LPS + sh-FOXO1+OE-NC and SAH + LPS + sh-FOXO1+OE-IL-10. Mice received scrambled shRNA (sh-NC) or sh-FOXO1 and overexpression lentivirus (Sangon Biotech, Shanghai) microinjection as described [25]. After 48 h, mice were treated with LPS, followed by SAH induction.

Experiment 4 Mice were divided into five groups (n = 5 per group): Sham, SAH, SAH + LPS, SAH + LPS + sh-NC and SAH + LPS + sh-USP19. Mice received scrambled shRNA (sh-NC) or sh-USP19 lentivirus (Sangon Biotech, Shanghai) microinjection as described [25]. After 48 h, mice were treated with LPS, followed by SAH induction.

Experiment 5 Mice were divided into six groups (n = 5 per group): Sham, SAH, SAH + LPS, SAH + LPS + sh-NC + OE-NC, SAH + LPS + sh-USP19+OE-NC and SAH + LPS + sh-USP19+OE-FOXO1. Mice received scrambled shRNA (sh-NC) or sh-USP19 and overexpression lentivirus (Sangon Biotech, Shanghai) microinjection as described [25]. After 48 h, mice were treated with LPS, followed by SAH induction.

2.2. Neurological evaluation

Neurological evaluation was performed as previously described [26]. Detailed information pertaining to Garcia Neuroscore was depicted in Table 2.

Table 1
Primers used in qRT-PCR.

Primer	Sequence 5′-3′
FOXO1 sense	CATTGCGGAAAGAGAGAGCC
FOXO1 anti-sense	AGGGGTTGCTGCTGAAATTG
IL-10 sense	GGTTGCCAAGCCTTATCGGA
IL-10 anti-sense	TTCAGCTTCTCACCCAGGGA
USP19 sense	AAGCTCCAAGACCAAGGTGT
USP19 anti-sense	AGCTCTGTCTAGGTCCTGGA
GAPDH sense	AGCCCAAGATGCCCTTCAGT
GAPDH anti-sense	CCGTGTTCCTACCCCCAATG

Table 2
Neurological evaluation using Garcia Scoring System.

Test	Scores			
	0	1	2	3
Spontaneous Activity (in cage for 5 min)	No movement	Barely moves position	Moves but does not approach at least three sides of cage	Moves and approaches at least three sides of cage
Spontaneous movements of all limbs	No movement	Slight movement of limbs	Moves all limbs but slowly	Move all limbs same as pre-SAH
Movements of forelimbs (outstretching while held by tail)	No outreaching	Slight outreaching	Outreach is limited and less than pre-SAH	Outreach same as pre-SAH
Climbing wall of wire cage		Fails to climb	Climbs weakly	Normal climbing
Reaction to touch on both side of trunk		No response	Weak response	Normal response
Response to vibrissae touch		No response	Weak response	Normal response

2.3. SAH grading

At 24 h after SAH surgery, SAH grading was performed by two independent investigators who were blinded to the treatment groups as described [27]. SAH mice with a SAH grade of ≤8 were excluded from this study. The SAH grade of each group was shown in Fig. S2A.

2.4. Measurement of brain edema

Mice were sacrificed at 24 h after SAH. The brains were harvested and rapidly weighed. After drying at 105 °C for 24 h, the dry weight of brains was recorded. The water content was calculated as follows: (wet weight-dry weight)/wet weight × 100%.

2.5. Hematoxylin Eosin (HE) staining

The brains were dissected, fixed and embedded in paraffin. After deparaffinization and rehydration, the slides were stained with HE as described [7]. Images were acquired under a microscope (Nikon, Tokyo. Japan).

2.6. Determination of blood-brain barrier (BBB) permeability

BBB permeability was determined by measuring Evans blue (EB) in the brain at 24 h after SAH. In brief, mice were anesthetized and injected with 4% EB dye (2.5 mL/kg) into the left femoral vein 1 h prior to the timepoint. EB extravasation in the brain (Ex620/Em680) was measured using a microplate reader (Thermo Fisher Scientific, Waltham, MA, USA). The vessel leakage was presented as μg/g of brain tissue.

2.7. Nissl staining

The brain tissues were cut into 16 μm slices and stained with 0.5% cresyl violet (Sigma-Aldrich). The slices were than dehydrated and rinsed with xylene. Images were acquired under a microscope (Nikon).

2.8. TUNEL assay

Cell apoptosis in the brain tissue was monitored using Click-iT Plus TUNEL assay kit (Invitrogen, Carlsbad, CA, USA). Briefly, the deparaffinized sections were fixed and permeabilized. The sections were incubated with TdT Reaction Buffer at 37 °C for 10 min, followed by the incubation with TdT reaction mixture 37 °C for 1 h. The slides were then incubated with Click-iT Plus TUNEL reaction cocktail at 37 °C for 30 min, and counterstained with DAPI. Images were acquired using a confocal microscope (Nikon).

2.9. ELISA assay

The serum levels of IL-6 (88-7064-22), IL-1β (88-7013-22) and TNF-α (88-7324-22) were detected using ELISA kits (Invitrogen). In brief, the whole blood was allowed to clot, and serum was collected after centrifugation. A450 was measured using a microplate reader (Thermo Fisher Scientific).

2.10. Cell culture, treatment and transfection

Mouse BV2 microglia cells and human neuroblastoma cell line SH-SY5Y cells were from ATCC (Manassas, MA, USA). BV2 and SH-SY5Y cells were grown in DMEM supplemented with 10% FBS (Gibco, Grand Island, NY, USA). All cells were maintained at 37 °C/5% CO_2. The *in vitro* SAH model was established as described [28]. Briefly, BV2 cells were seeded in a Transwell insert (Corning, Corning, NY, USA), and treated with 10 μM oxyhemoglobin and co-culturing with SH-SY5Y cells for 24 h. The full-length of FOXO1 or USP19 were cloned into pcDNA3.1 vector (Invitrogen). SH-SY5Y cells were transfected with sh-FOXO1 (Sangon Biotech, Shanghai), OE-FOXO1, OE-USP19 or corresponding control using Lipofectamine 3000 reagent (Invitrogen).

2.11. Immunofluorescence (IF)

Microglial were fixed with 4% PFA and permeabilized with 0.3% Triton X-100. The slides were blocked with 1% BSA, and incubated with anti-CD16/CD32 (1:100, ab171202, Abcam, Cambridge, UK), anti-CD206 (1:100, PA5-101657, Invitrogen), anti-IBA1 (1:100, ab283319, Abcam) or anti-FOXO1 (1:100, ab52857) antibodies at 4 °C overnight. This is followed by the incubation with Alexa Fluor 488- and Alexa Fluor 555-conjugated secondary antibodies. The slides were then mounted with Prolong Gold antifade mountant (Invitrogen) and observed under a confocal microscope (Nikon). To check for the non-specific staining, primary antibody was omitted as a negative control. No signal was detected without the incubation of primary antibody (Fig. S3B).

2.12. Western blot

Protein lysates were prepared in RIPA lysis buffer (Pierce, Rockford, IL, USA) and quantified using Bradford reagent (Pierce). Proteins were separated by gel electrophoresis and transferred onto NC membrane. After blocking, the blots were incubated with primary antibody at 4 °C overnight, followed by the incubation with corresponding secondary antibody. Signals were detected using a ECL kit (Pierce). Antibodies used in Western blot: anti-SOD (1:5000, ab13498), anti-GPx (1:1000, ab22604), anti-USP19 (1:1000, ab93159), anti-FOXO1 (1:1000, ab52857), anti-IL-10 (1:1000, ab33471), anti-IL-10R1 (1:1000, ab89883), anti-MMP9 (1:1000, ab38898) and anti-β-actin antibodies (1:2000, ab8226, Abcam).

2.13. qRT-PCR

Total RNA was isolated using Trizol (Invitrogen), and reverse transcribed using Advantage RT for PCR kit (TaKaRa, Dalian, China). qRT-PCR was conducted using iQTM SYBR Green Supermix (Bio-Rad, Hercules, CA, USA) and calculated using $2^{-\Delta\Delta CT}$ method. Primers used in qRT-PCR were listed in Table 1.

2.14. Dual luciferase reporter assay

The wild-type or mutated IL-10 promoter region was cloned into pGL-3 vector (Promega, Madison, WI, USA). FOXO1 overexpression construct,

sh-FOXO1 or corresponding control and luciferase construct were co-transfected into H293T cells. Luciferase activity was measured using Dual Luciferase Reporter System (Promega) at 48 h post-transfection.

2.15. Chromatin immunoprecipitation (ChIP) assay

ChIP assay was conducted using Pierce Agarose ChIP Kit (Pierce). In brief, SH-SY5Y cells were cross-linked with 1% formaldehyde, and subjected to lysis and MNase digestion. The digested chromatin was then incubated with anti-FOXO1 antibody (2 μg, MA5-17078, Invitrogen) or normal mouse IgG at 4 °C overnight. The enriched DNA was purified and analyzed by qRT-PCR.

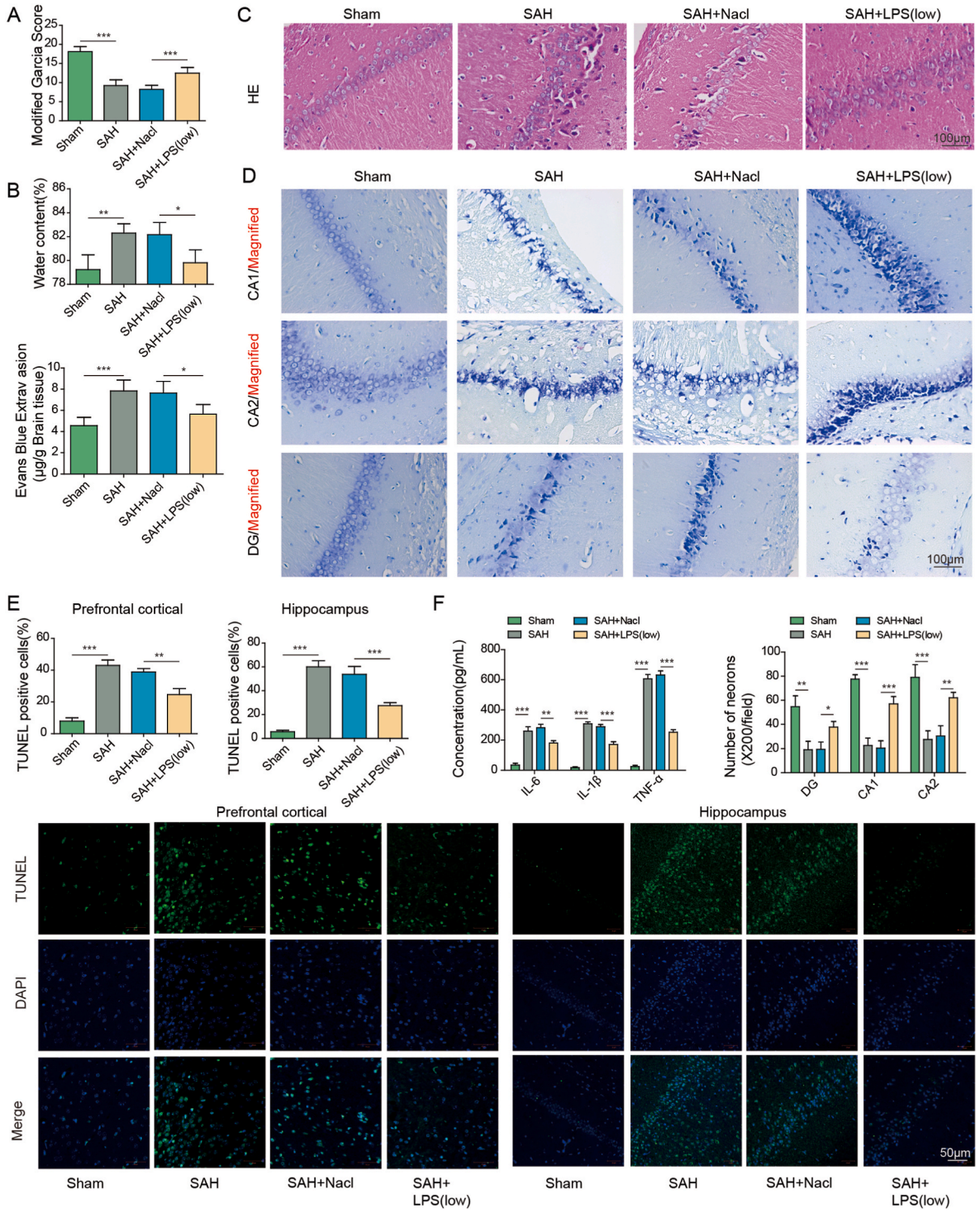

Fig. 1. Low-dose LPS alleviates early brain injury after SAH. (A) Neurobehavioral deficits were evaluated by Garcia Neuroscore. (B) Brain water content was assessed by wet-dry weight method. (C) The histological changes and BBB permeability were measured by HE staining and EB permeability assay, respectively. (D) Damage in the hippocampus was assessed by Nissl staining. (E) Apoptosis of prefrontal cortical and hippocampal neurons was detected by TUNEL assay. Scale bar. (F) The secretion of cytokines was detected by ELISA assay. (G) The expression of IBA1 and M1/M2 markers were detected by IF with quantitative analysis. (H) The protein levels of SOD, Gpx, USP19, FOXO1, IL-10, IL-10R1 and MMP9 were determined by Western blot. *, $P < 0.05$; **, $P < 0.01$; ***, $P < 0.001$.

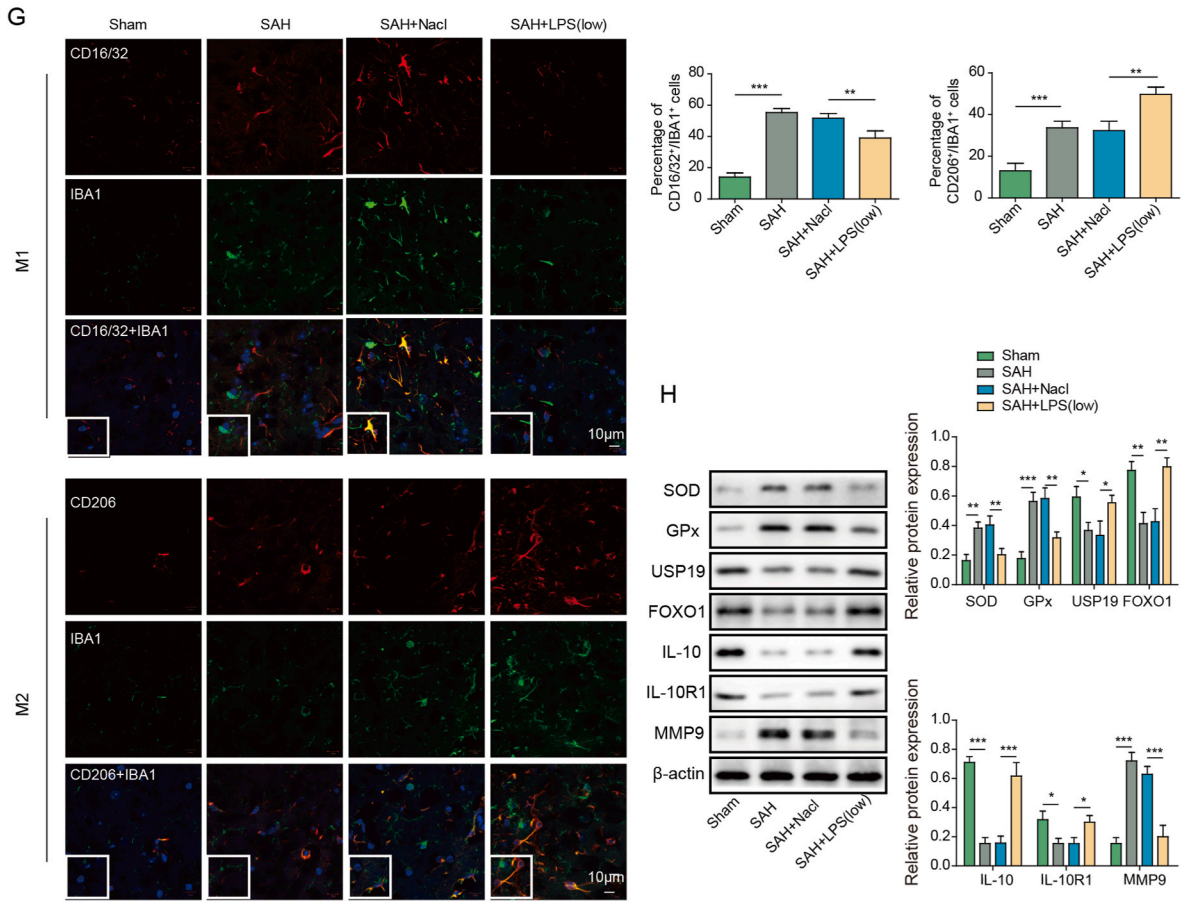

Fig. 1. (*continued*).

2.16. Co-immunoprecipitation (co-IP)

SH-SY5Y cells were lysed using IP lysis buffer (Pierce). Cells were transfected Sh-USP19 which were treated with the Proteasome inhibitor MG132(10 μM, Merck Millipore) for 4 h. Antibody against FOXO1 (2 μg, MA5-14846, Invitrogen) or normal rabbit IgG was incubated with cell lysates at 4 °C overnight. Protein A/G agarose (Pierce) was then added to enrich the complexes. After elution, the immunoprecipitated complexes were then analyzed by Western blot.

2.17. Flow cytometry

Cell apoptosis was monitored using Annexin V apoptosis detection kit (Invitrogen). Briefly, SH-SY5Y cells were resuspended with Binding Buffer, and stained with 5 μL Annexin V-FITC and 5 μL PI. Data were acquired on a flow cytometer (BD Biosciences, San Jose, CA, USA).

2.18. Statistical analysis

Data were analyzed using SPSS 22.0. One-way ANOVA or Student's *t*-test was conducted to assess the differences. The observers were blinded to treatment groups. $P < 0.05$ was regarded statistically significant.

3. Results

3.1. Low-dose LPS alleviates early brain injury after SAH

To investigate the protective effects of low-dose LPS on early brain injury after SAH, SAH mice were pre-treated with saline or LPS. As presented in Fig. 1A, Garcia neurobehavioral scoring showed that SAH mice exhibited a remarkably decreased neuroscore, while low-dose LPS preconditioning led to a rebound of neuroscore in SAH mice. Detailed information pertaining to Garcia Neuroscore was depicted in Table 2. Brain edema was markedly induced by SAH as detected by wet-dry weight method, whereas brain water content was decreased by low-dose LPS preconditioning (Fig. 1B). Moreover, HE staining and EB permeability assay revealed that low-dose LPS alleviated brain injury and BBB disruption after SAH (Fig. 1C). Nissl staining showed severe damage in the hippocampal region in SAH mice in which cells showed dissolution and pyknosis of chromatin, while low-dose LPS significantly reduced the injury in the hippocampus (Fig. 1D). Consistently, TUNEL assay further revealed that apoptosis of prefrontal cortical and hippocampal neurons after SAH was reduced by low-dose LPS (Fig. 1E). The increased secretion of IL-6, IL-1β and TNF-α after SAH were attenuated by low-dose LPS as detected by ELISA assay (Fig. 1F). In addition, the morphologies of IBA1-positive microglia in sham, SAH, SAH + Nacl and SAH + LPS groups were compared by IF staining. As presented in Fig. S3A, the activated microglia in SAH group exhibited increased cell volume and more branching, compared with microglia in sham group. Low-dose LPS weakened the activation of M1 microglia induced by SAH, while SAH + LPS group increased the expansion and branching of M2 microglia (Fig. S3A). Interestingly, IF staining also showed that the increased expression of M1 marker CD16/32, as well as the decreased expression of M2 marker CD206 in microglia after SAH, were reversed by low-dose LPS (Fig. 1G), indicating that low-dose LPS promoted M2 microglia polarization. Furthermore, Western blot showed that low-dose LPS exerted protective effects on oxidative stress in which SAH-induced SOD and Gpx were attenuated by low-dose LPS (Fig. 1H). Additionally, low-dose LPS counteracted SAH-decreased USP19, FOXO1, IL-10 and IL-10R1, along with SAH-increased MMP9 in mouse brain (Fig. 1H). Collectively, these findings suggest that

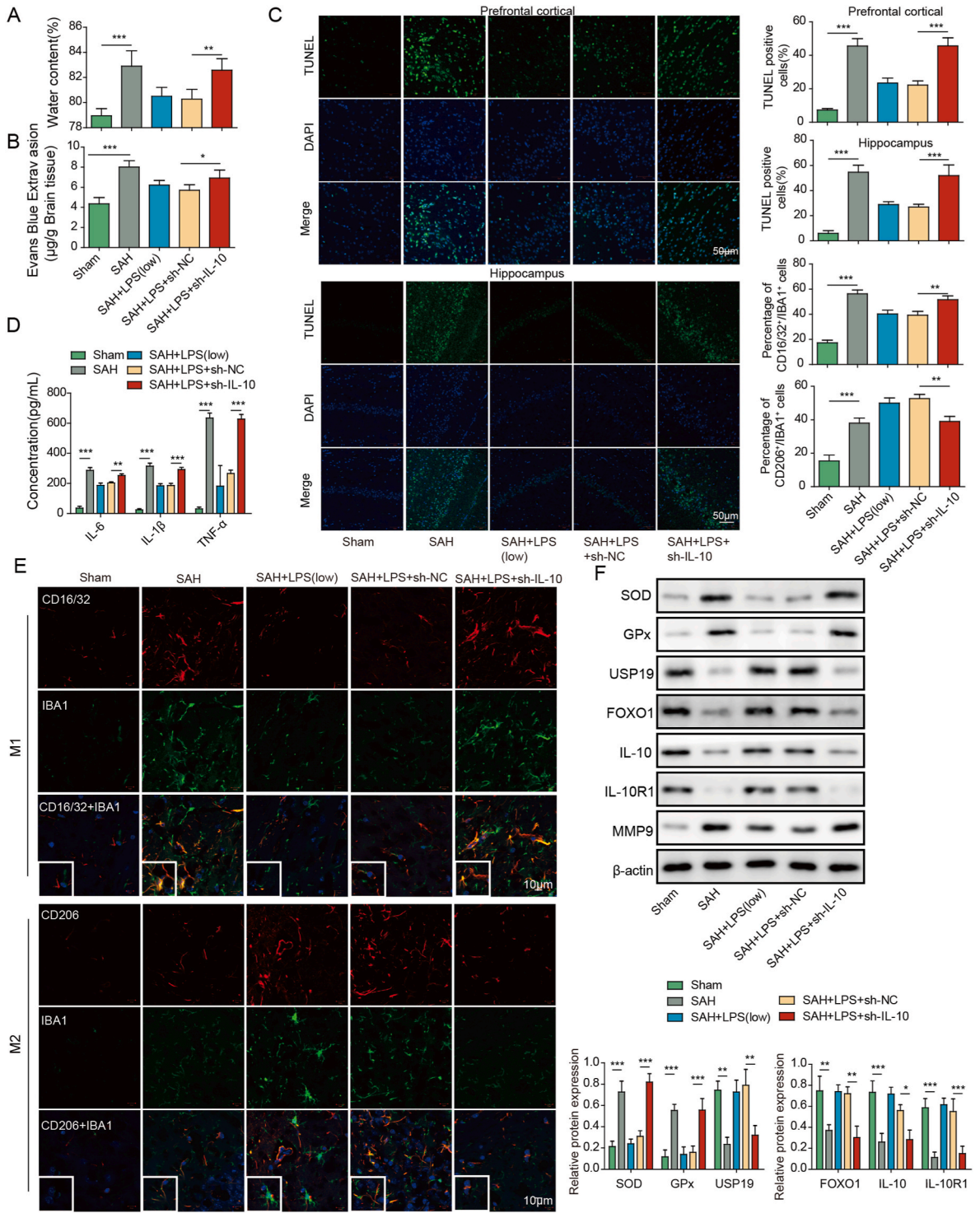

Fig. 2. Low-dose LPS alleviates early brain injury after SAH via modulating microglial M1/M2 polarization by IL-10/IL-10R1 signaling. (A) Brain water content was assessed by wet-dry weight method. (B) BBB permeability were measured by EB permeability assay. (C) Apoptosis of prefrontal cortical and hippocampal neurons was detected by TUNEL assay. Scale bar. (D) The secretion of cytokines was detected by ELISA assay. (E) The expression of IBA1 and M1/M2 markers were detected by IF with quantitative analysis. Scale bar. (F) The protein levels of SOD, Gpx, USP19, FOXO1, IL-10, IL-10R1 and MMP9 were determined by Western blot. *, $P < 0.05$; **, $P < 0.01$; ***, $P < 0.001$.

low-dose LPS protects against early brain injury after SAH.

3.2. Low-dose LPS alleviates early brain injury after SAH via modulating microglial M1/M2 polarization by IL-10/IL-10R1 signaling

To further delineate the mechanism underlying low-dose LPS alleviated brain injury after SAH, IL-10 knockdown study was conducted. Wet-dry weight method and EB permeability assay showed that the protective effects of low-dose LPS on SAH-induced brain edema and BBB disruption were reversed by IL-10 knockdown (Fig. 2A and B). In addition, silencing of IL-10 counteracted low-dose LPS-decreased apoptosis of prefrontal cortical and hippocampal neurons after SAH (Fig. 2C). ELISA assay further revealed that low-dose LPS-decreased secretion of pro-inflammatory cytokines were rebounded by IL-10

knockdown (Fig. 2D). As presented in Fig. 2E, the effects of low-dose LPS on microglial M1/M2 polarization were also reversed by IL-10 silencing. As anticipated, silencing of IL-10 successfully decreased IL-10 level in brain tissues, compared with corresponding control (Fig. 2F). IL-10 knockdown also attenuated the effects of low-dose LPS on the expression of SOD, GPx, USP19, FOXO1, IL-10R1 and MMP9 in mouse brain (Fig. 2F). These data indicate that IL-10/IL-10R1 signaling plays a key role in mediating the protective effects of low-dose LPS in SAH mice.

3.3. FOXO1 acts as a transcriptional activator of IL-10

Bioinformatics analysis based on JASPAR database predicted two (site 1 and site 2) putative binding site between FOXO1 and IL-10 promoter (Fig. 3A and B). Dual luciferase assay showed that co-transfection of wild-type IL-10 reporter (wt) and FOXO1 overexpression construct (OE-FOXO1) resulted in a dramatic induction of luciferase activity (Fig. 3C). In contrast, the simultaneous mutation of two sites (mt1) of IL-10 reporter gene eliminated the change of luciferase activity mediated by OE-FOXO1, while the luciferase activity mediated by OE-FOXO1 was still significantly different after only one site (mt2 or mt3) of IL-10 was mutated (Fig. 3C). Therefore, we speculated that FOXO1 regulated transcription by acting on two sites in the promoter region of IL-10. CHIP assay further confirmed the direct association between FOXO1 and IL-10 promoter in which antibody against FOXO1 successfully enriched IL-10 promoter (Fig. 3D). As expected, qRT-PCR and Western blot showed that OE-FOXO1 increased FOXO1 and IL-10 expression, and sh-FOXO1 decreased FOXO1 and IL-10 expression in SH-SY5Y cells (Fig. 3E). These findings indicate that FOXO1 positively regulates IL-10 expression at transcriptional level.

3.4. Low-dose LPS alleviates early brain injury after SAH via modulating microglial M1/M2 polarization by FOXO1/IL-10/IL-10R1 axis

To study the function of FOXO1/IL-10 axis in SAH, *in vivo* functional experiments were next carried out. In consistent with the *in vitro* findings, silencing of FOXO1 decreased the expression of FOXO1 and IL-10 in mouse brain tissues (Fig. 4A and B). IL-10 overexpression successfully increased IL-10 expression, but caused no change of FOXO1 level at both mRNA and protein levels (Fig. 4A). As shown in Fig. 4C-D, overexpression of IL-10 abrogated the effects of FOXO1 silencing on brain injury and BBB integrity. The effects of FOXO1 silencing on apoptosis of prefrontal cortical and hippocampal neurons after SAH were also abolished by IL-10 overexpression as detected by TUNEL assay. ELISA assay and IF staining further revealed that overexpression of IL-10 reversed the effects of FOXO1 knockdown on inflammation and microglial M1/M2 polarization. In addition, IL-10 overexpression attenuated sh-FOXO1-induced changes on SOD and Gpx expression in mouse brain tissues (Fig. 4H). Together, these data suggest that low-dose LPS

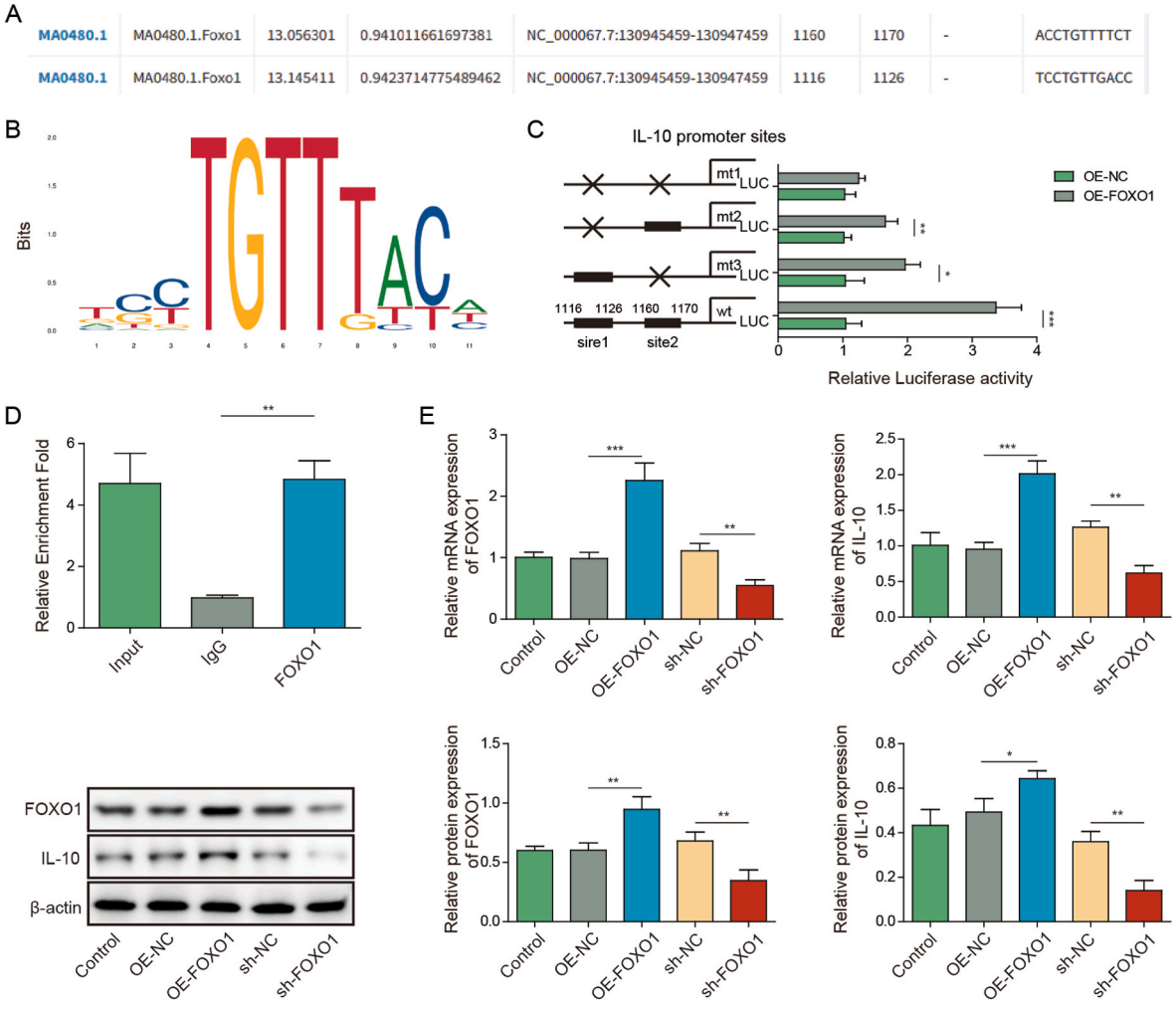

Fig. 3. FOXO1 acts as a transcriptional activator of IL-10. (A) The putative binding site between FOXO1 and IL-10 promoter. (B) Schematic drawing depicting the potential mechanism of FOXO1-regulated IL-10 expression. (C) Luciferase activity was measured by dual luciferase assay. (D) The direct association between FOXO1 and IL-10 promoter was detected by ChIP assay. Normal IgG served as a negative control. (E) The mRNA and protein levels of FOXO1 and IL-10 were detected by qRT-PCR and Western blot, respectively. *, $P < 0.05$; **, $P < 0.01$; ***, $P < 0.001$.

alleviates early brain injury after SAH via FOXO1/IL-10/IL-10R1 axis.

3.5. USP19 regulates microglial M1/M2 polarization by deubiquitinating FOXO1 to activate IL-10/IL-10R1 signaling

As shown in Figues. 4A and 4B, we found an interesting phenomenon. There was no significant difference in the mRNA level of FOXO1 between sham-operated and SAH model mice, but there was a significant difference in protein level (Fig. 4A and B). In order to further find out the possible protein level modification of FOXO1 in SAH, we predicted the existence of ubiquitination modification of FOXO1 protein by UbiBrowser 2.0 (http://ubibrowser.bio-it.cn/ubibrowser_v3/). We predicted the possible ubiquitination enzymes of FOXO1 from mouse and human respectively. Then, we found that there were 12 common

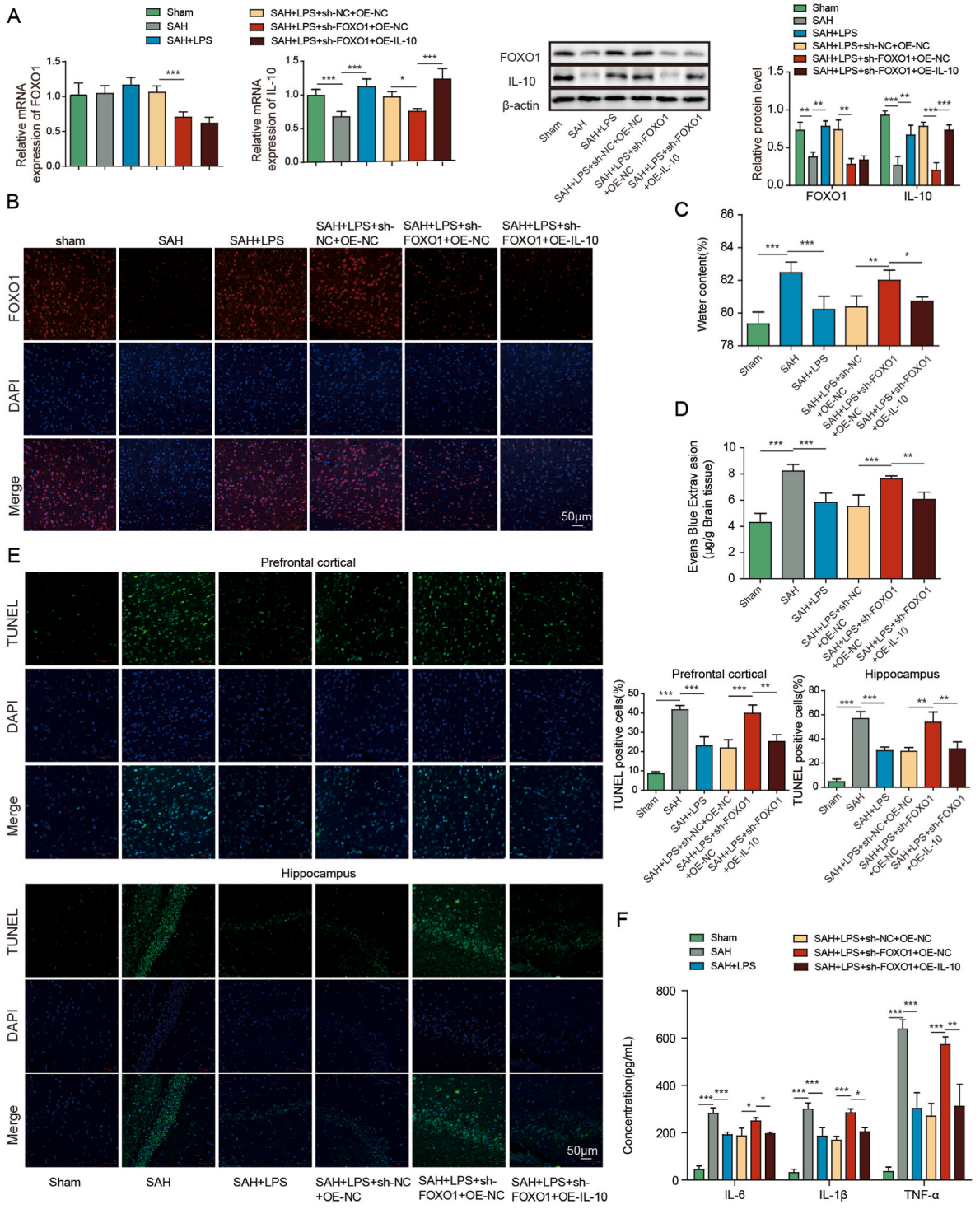

Fig. 4. Low-dose LPS alleviates early brain injury after SAH via modulating microglial M1/M2 polarization by FOXO1/IL-10/IL-10R1 axis. (A) The mRNA and protein levels of FOXO1 and IL-10 were detected by qRT-PCR and Western blot, respectively. (B) The expression of FOXO1 was detected by IF. (C) Brain water content was assessed by wet-dry weight method. (D) BBB permeability were measured by EB permeability assay. (E) Apoptosis of prefrontal cortical and hippocampal neurons was detected by TUNEL assay. (F) The secretion of cytokines was detected by ELISA assay. (G) The expression of IBA1 and M1/M2 markers were detected by IF with quantitative analysis. (H) The protein levels of SOD and Gpx were determined by Western blot. *, $P < 0.05$; **, $P < 0.01$; ***, $P < 0.001$.

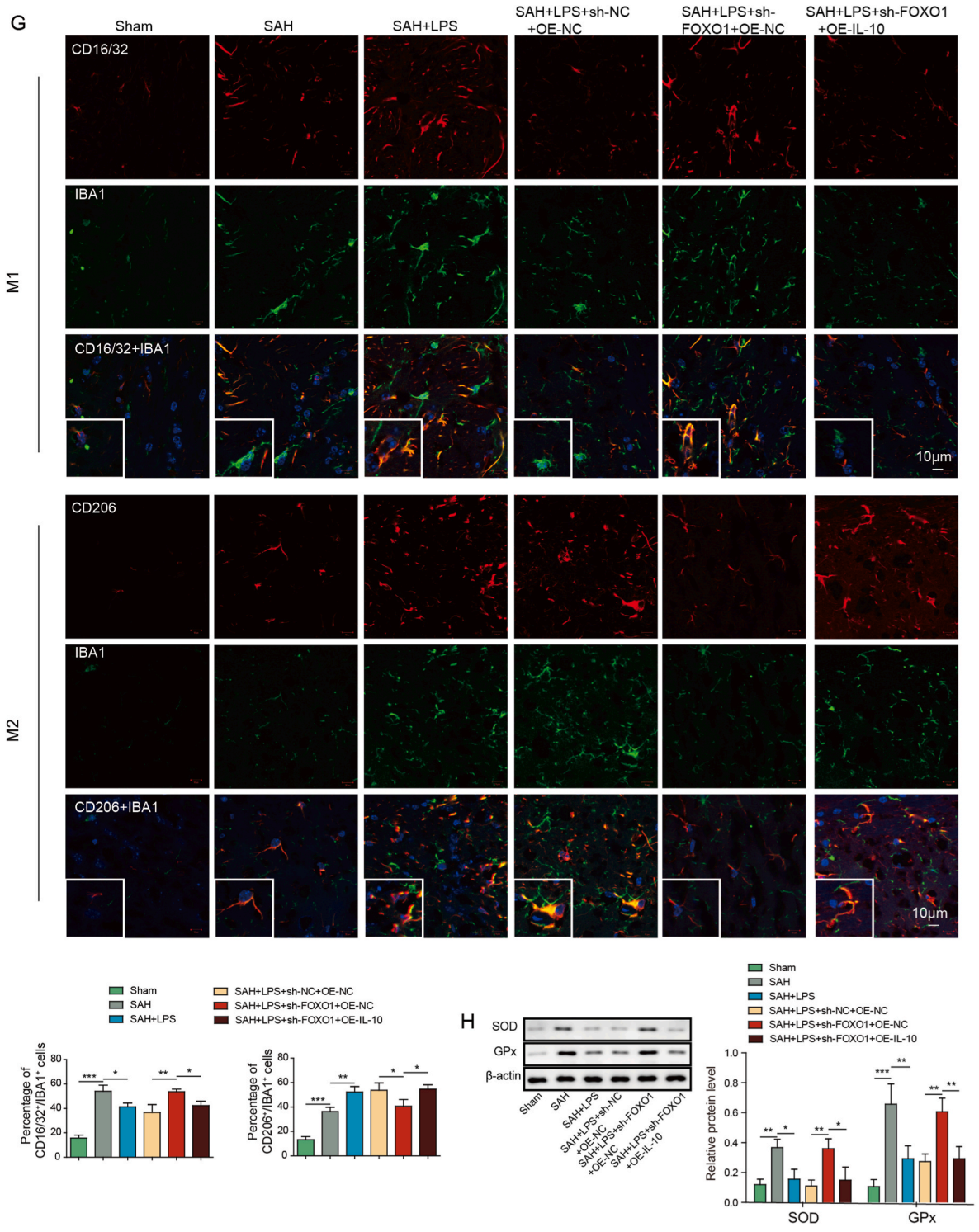

Fig. 4. (*continued*).

ubiquitination enzymes by comparing Venn diagram (Fig. S1A). Then, we detected the expression changes of 12 ubiquitination enzymes in the brain tissue of SAH mice, and we were surprised to find that USP19 was significantly down-regulated in SAH (Fig. S1B).

We next sought to investigate the regulatory mechanism between USP19 and FOXO1/IL-10/IL-10R1 axis. As presented in Fig. 5A, USP19 overexpression led to induction of USP19, FOXO1, IL-10 and IL-10R1 in SH-SY5Y cells. By contrast, silencing of USP19 exerted opposite effects on the expression of these proteins (Fig. 5A). co-IP revealed that lack of USP19 increased the ubiquitination of FOXO1 in SH-SY5Y cells (Fig. 5B).

Functional studies were next performed in the *in vitro* SAH model. SH-SY5Y cells were co-cultured with BV2 cells and treated with oxyhemoglobin (OHb) (Fig. 5C). IF staining revealed that overexpression of USP19 promoted microglial M2 polarization in which the percentage of $CD206^{+}IBA1^{+}$ cells were remarkably increased in OHb+OE-USP19 group (Fig. 5D). Additionally, Annexin V-FITC/PI staining showed that USP19 overexpression inhibited OHb-induced apoptosis of SH-SY5Y cells (Fig. 5E). As expected, OHb-induced inflammation and oxidative stress in SH-SY5Y cells were also attenuated by USP19 overexpression as detected by ELISA assay and Western blot, respectively (Fig. 5F and G).

Collectively, these data suggest that USP19 regulates microglial M1/M2 polarization via FOXO1/IL-10/IL-10R1 axis *in vitro*.

3.6. Low-dose LPS upregulates UPS19 to modulate microglial M1/M2 polarization in SAH mice

In order to delineate the role of USP19 in SAH mice, *in vivo* knockdown studies were conducted. Intriguingly, SAH-decreased USP19 expression was reversed by low-dose LPS, and sh-USP19 further attenuated the effect of low-dose LPS on USP19 expression in mouse brain (Fig. 6A). Similarly, USP19 knockdown abrogated the protective effects of low-dose LPS on brain edema and BBB integrity (Fig. 6B and C). TUNEL assay further showed that low-dose LPS-decreased apoptosis of prefrontal cortical and hippocampal neurons after SAH was

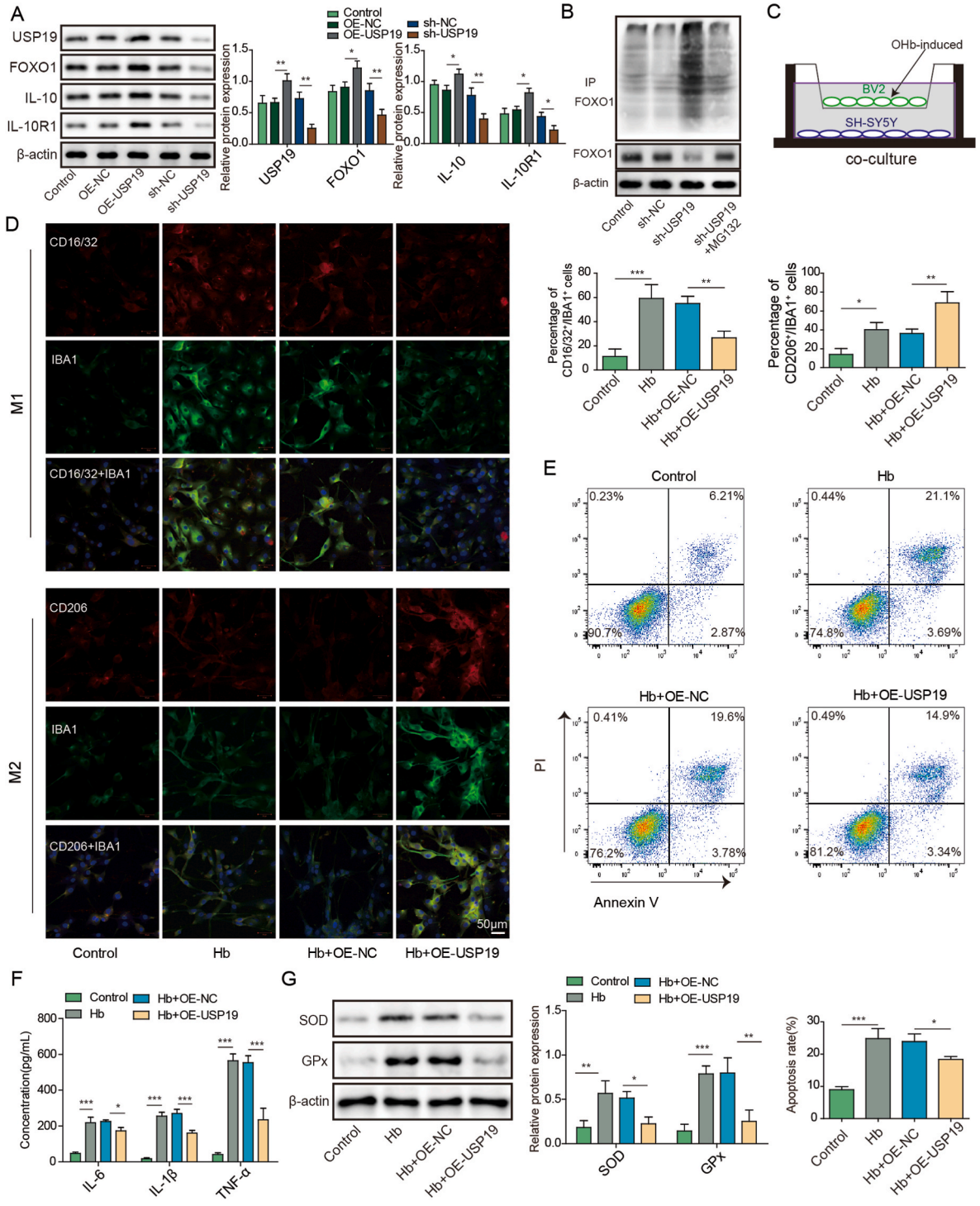

Fig. 5. USP19 regulates microglial M1/M2 polarization by deubiquitinating FOXO1 to activate IL-10/IL-10R1 signaling. (A) The protein levels of USP19, FOXO1, IL-10 and IL-10R1 were detected by Western blot. (B) The ubiquitination of FOXO1 was monitored by co-IP. (C) SH-SY5Y cells were co-cultured with BV2 cells. (D) The expression of IBA1 and M1/M2 markers were detected by IF with quantitative analysis. (E) The apoptosis of SH-SY5Y cells were assessed by Annexin V-FITC/PI staining. (F) The secretion of cytokines in SH-SY5Y cells was detected by ELISA assay. (G) The protein levels of SOD and Gpx in SH-SY5Y cells were determined by Western blot. *, $P < 0.05$; **, $P < 0.01$; ***, $P < 0.001$.

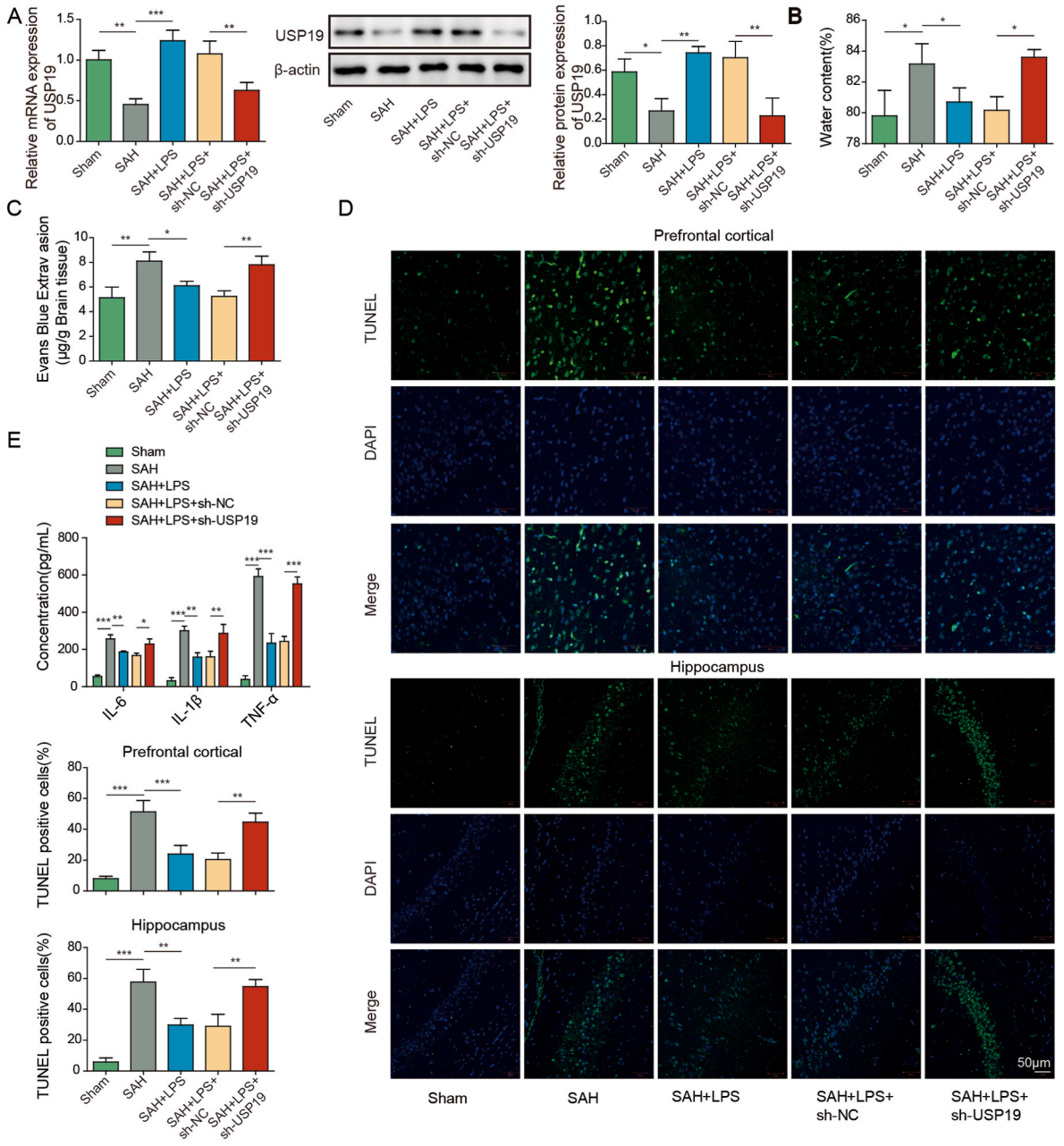

Fig. 6. Low-dose LPS upregulates UPS19 to modulate microglial M1/M2 polarization in SAH mice. (A) The mRNA and protein levels of USP19 were detected by qRT-PCR and Western blot, respectively. (B) Brain water content was assessed by wet-dry weight method. (C) BBB permeability were measured by EB permeability assay. (D) Apoptosis of prefrontal cortical and hippocampal neurons was detected by TUNEL assay. (E) The secretion of cytokines was detected by ELISA assay. (F) The expression of IBA1 and M1/M2 markers were detected by IF with quantitative analysis. (G) The protein levels of SOD and Gpx were determined by Western blot. *, $P < 0.05$; **, $P < 0.01$; ***, $P < 0.001$.

counteracted by USP19 silencing (Fig. 6D). Moreover, the effects of low-dose LPS on inflammation and microglial M1/M2 polarization were also reversed by USP19 knockdown (Fig. 6E and F). Furthermore, low-dose LPS-decreased expression of SOD and Gpx were rebound in SAH + LPS (low)+sh-USP19 group (Fig. 6G), indicating that the protective effect of low-dose LPS on oxidative stress was abolished by USP19 knockdown. These data indicate that low-dose LPS protects against SAH-induce brain injury via upregulating USP19.

3.7. Low-dose LPS upregulates USP19 to modulate microglial M1/M2 polarization via FOXO1/IL-10/IL-10R1 signaling in SAH mice

The function of USP19/FOXO1/IL-10/IL-10R1 signaling was validated in SAH mice by gain- and loss-of function experiments. In line with the *in vitro* findings, silencing of USP19 reduced the expression of USP19, FOXO1, IL-10 and IL-10R1 in mouse brain (Fig. 7A). Overexpression of FOXO1 has no effect on USP19 level, but it resulted in rebounds of FOXO1, IL-10 and IL-10R1 (Fig. 7A). FOXO1 overexpression attenuated the effects of sh-USP19 on brain edema, histological damage and BBB integrity in mouse brain, compared with SAH + LPS (low)+sh-USP19 group (Fig. 7B and C). TUNEL assay further showed that the

F

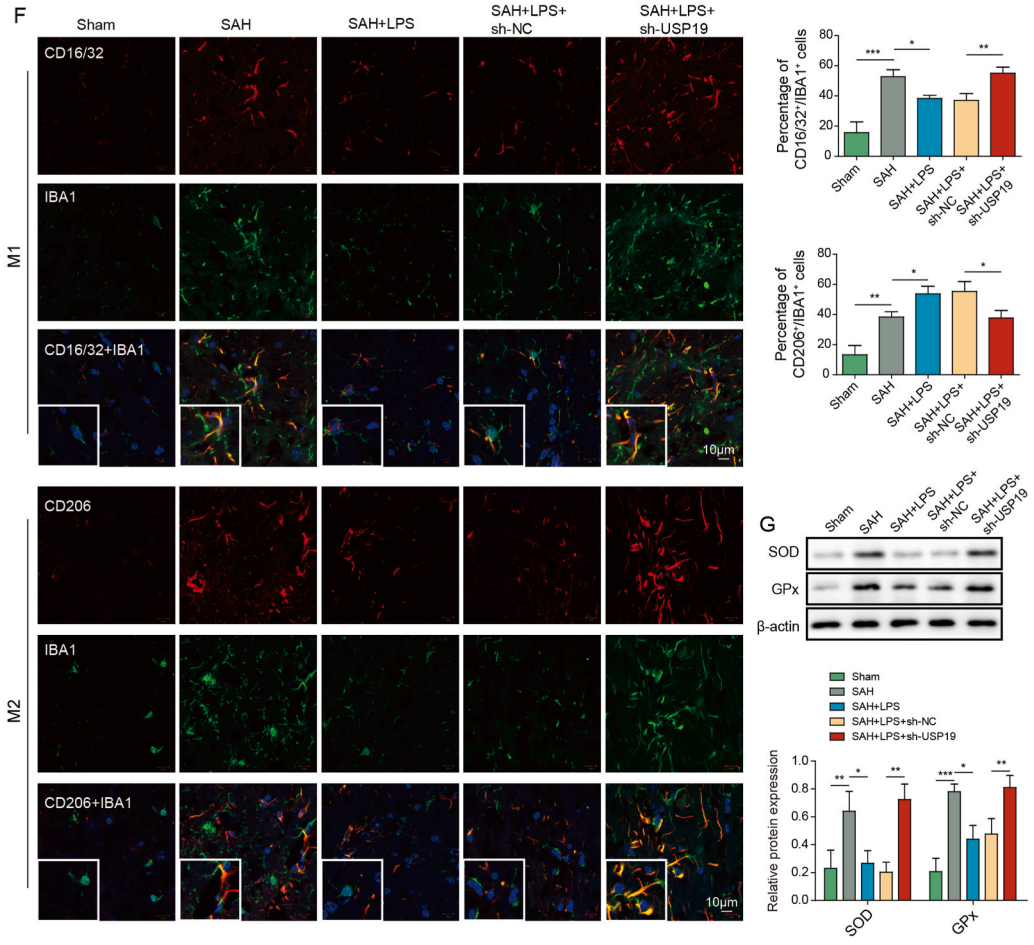

Fig. 6. (*continued*).

effect of USP19 knockdown on apoptosis of prefrontal cortical and hippocampal neurons in SAH mice was reversed by FOXO1 overexpression (Fig. 7D). ELISA assay revealed that sh-USP19-increased secretion of IL-6, IL-1β and TNF-α were abolished by OE-FOXO1 (Fig. 7E). As expected, IF staining and Western blot further showed that FOXO1 overexpression counteracted the effects of sh-USP19 on microglial M1/M2 polarization and oxidative stress in SAH mice (Fig. 7F and G). These findings indicate that low-dose LPS exerts neuroprotective effects via upregulating USP19 to activate FOXO1/IL-10/IL-10R1 signaling in SAH mice.

4. Discussion

SAH is a devastating type of stroke with ~30% mortality rate [29]. Increasing evidence supports that EBI plays a critical role in the clinical outcomes of patients with SAH [2,30]. In the current study, we found that low-dose LPS exerted neuroprotective effects via modulating microglial M1/M2 polarization by IL-10/IL-10R1 signaling. In microglia, FOXO1 positively regulated IL-10 expression at the transcriptional level, and USP19 was implicated in the deubiquitination of FOXO1. Functional studies revealed that low-dose LPS ameliorated EBI after SAH by modulating microglial polarization via USP19/FOXO1/IL-10/IL-10 R1 axis.

Microglia can switch to either M1 (pro-inflammatory) or M2 (anti-inflammatory) polarized phenotypes [31]. Activation and early M1 polarization of microglia are observed after SAH [32]. Previous studies have illustrated that low-dose LPS improves SAH-induced neurodysfunction, BBB leakage, brain edema and apoptosis of neurons by decreasing MMP9 and caspase 3, as well as TLR4 signaling activation [6,7]. Consistently, our data confirmed the neuroprotective role of low-dose LPS after SAH. More importantly, we reported that low-dose LPS facilitated the M2 polarization of microglia, accompanied with decreased secretion of pro-inflammatory cytokines and oxidative stress markers. In line with the previous reports, low-dose LPS also decreased MMP9 expression [6,7], along with the upregulation of USP19, FOXO1, IL-10 and IL-10R1. Knockdown studies further supported that IL-10 acted as a functional effector in low-dose LPS-regulated microglial polarization following SAH. In addition to MMP9-associated signaling, our findings unraveled a novel regulatory axis underlying the neuroprotective effects of low-dose LPS after SAH.

Low-dose LPS suppresses cerebral I/R-induced neuronal cell apoptosis via PI3K/Akt/FOXO1 signaling. In particular, low-dose LPS leads to rebounds of FOXO1 and p-FOXO1 in I/R model rats [19]. Another study has reported that LPS also induces FOXO1 in M-CSF-derived macrophage [33]. Similarly, we reported that low-dose LPS reversed SAH-mediated downregulation of FOXO1 and IL-10. Mechanistically, FOXO1 positively regulated IL-10 via direct binding to its promoter in microglia which is consistent with a study demonstrating FOXO1 is enriched in IL-10 promoter in macrophages [33]. FOXO1 facilitates M2 polarization of Microglia by increasing IL-10

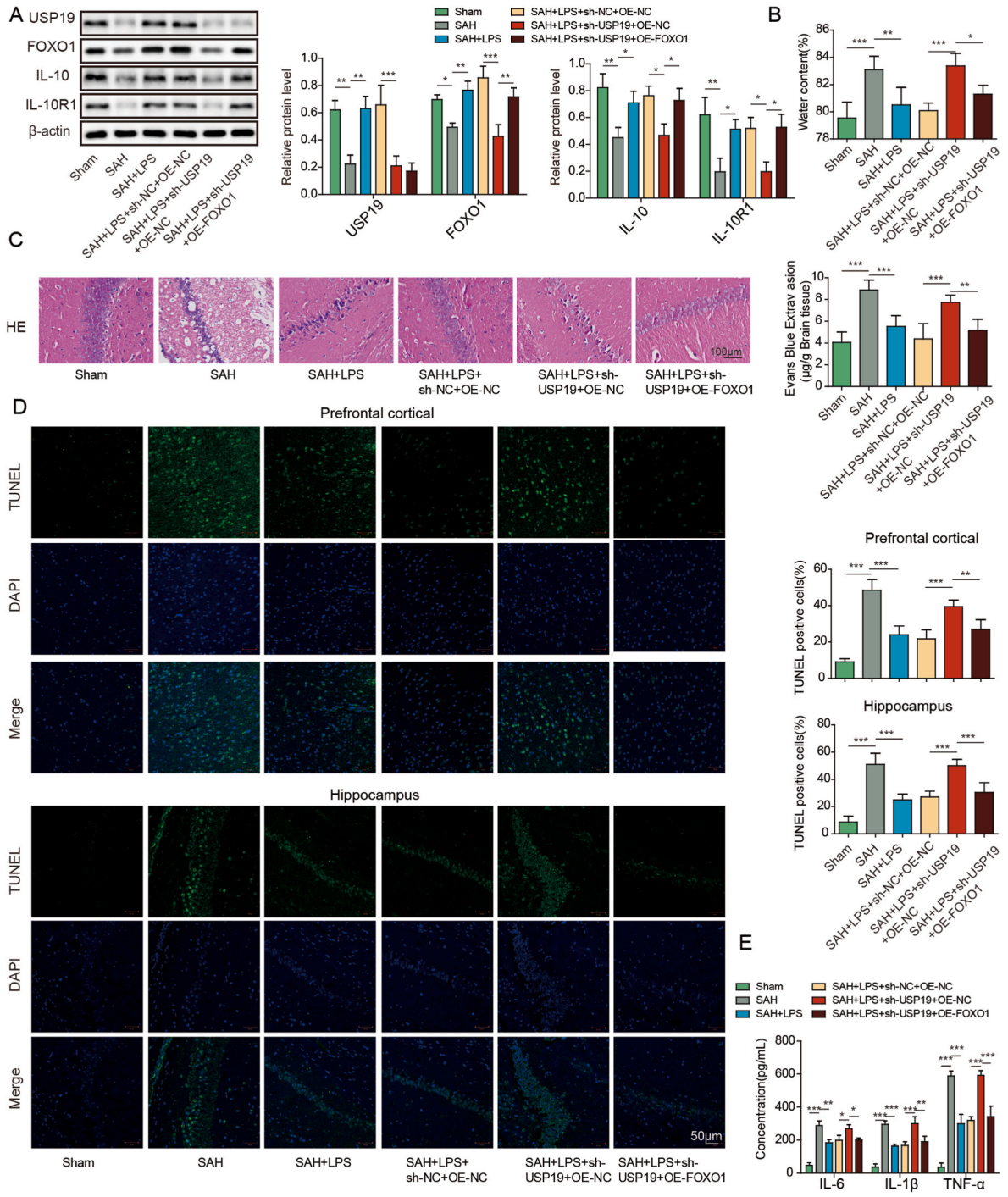

Fig. 7. Low-dose LPS upregulates USP19 to modulate microglial M1/M2 polarization via FOXO1/IL-10/IL-10R1 signaling in SAH mice. (A) The protein levels of USP19, FOXO1, IL-10 and IL-10R1 were detected by Western blot. (B) Brain water content was assessed by wet-dry weight method. (C) The histological changes and BBB permeability were measured by HE staining and EB permeability assay, respectively. (D) Apoptosis of prefrontal cortical and hippocampal neurons was detected by TUNEL assay. (E) The secretion of cytokines was detected by ELISA assay. (F) The expression of IBA1 and M1/M2 markers were detected by IF with quantitative analysis. (G) The protein levels of SOD and Gpx were detected by Western blot. *, $P < 0.05$; **, $P < 0.01$; ***, $P < 0.001$.

expression. In accordance with this report, our findings revealed that FOXO1/IL-10/IL-10R1 signaling played a pivotal role in low-dose LPS-mediated M2 polarization of microglia. Interestingly, IL-10 increased FOXO1 expression in differentiating iTregs [34]. It is of interest to investigate whether there is a regulatory loop between FOXO1 and IL-10 in SAH model. Accumulating evidence supports the neuroprotective role of IL-10 in ischemic stroke, however, the function of IL-10 in SAH is less clear [35]. Further study is needed to delineate the downstream signaling of IL-10 in SAH model.

USP19 knockout mice are more susceptible to the damage of inflammation, suggesting the crucial role of USP19 in the inflammatory response [15]. Recent study has demonstrated that USP19 negatively regulates TNF-α- and IL-1β-activated NF-κB signaling via deubiquinating TAK1 [14]. Additionally, USP19 is implicated in the deubiquitination of TRIF, thus inhibiting TLR3/4 signaling [15]. Our study reported that lack of USP19 reversed the protective effect of low-dose LPS on

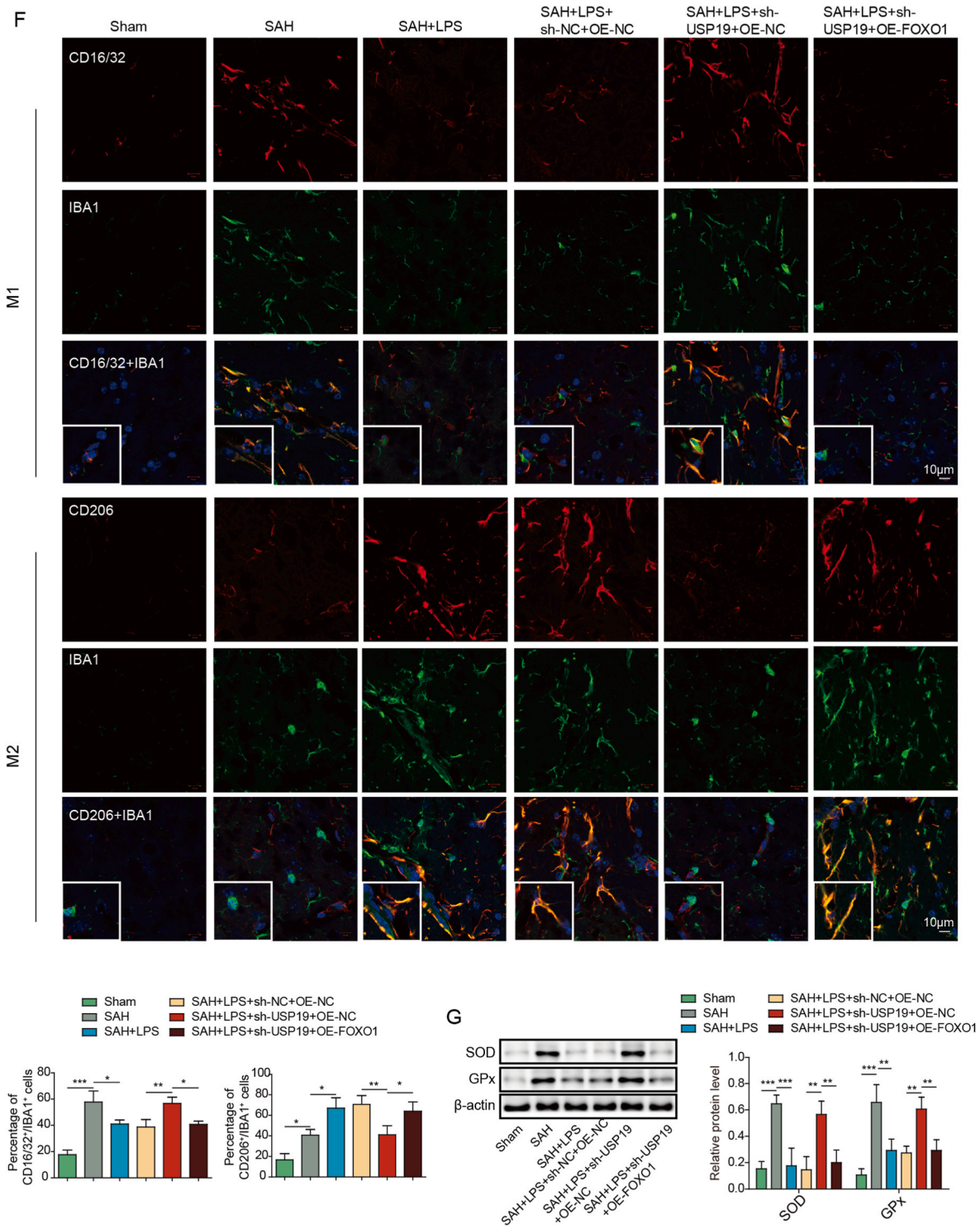

Fig. 7. (*continued*).

inflammation in SAH mice, as well as other neurological parameters. Besides being a downstream molecule of PI3K/Akt signaling, FOXO1 was identified as a substrate of USP19 in this study. USP19 was required for the deubiquination of FOXO1, and contributed to microglial polarization, apoptosis, inflammation and oxidative stress *in vitro*. The function of USP19/FOXO1/IL-10/IL-10R1 signaling was also validated *in vivo*.

Mounting evidence supports the crucial role of oxidative stress in SAH [36,37]. It worth noting that low-dose LPS counteracted SAH-increased SOD and GPx expression in brain tissues, supporting the protective effect of low-dose LPS on oxidative stress. Moreover, gain- and lost-of function experiments revealed that USP19/FOXO1/IL-10/IL-10R1 axis also contributed to low-dose LPS-mediated neuroprotection on oxidative stress. A recent study has illustrated that SIRT1 facilitates M2 microglial polarization through modulating ROS-NLRP3 inflammasome signaling after SAH [38], suggesting the crosstalk between microglial polarization and oxidative stress in SAH. The neuroprotective role of low-dose LPS on oxidative stress required further investigation in the future study, and it might be a promising antioxidant therapy for SAH.

In conclusion, we demonstrated that low-dose LPS protected against EBI after SAH by promoting microglial M2 polarization via USP19/FOXO1/IL-10/IL-10R1 signaling.

Data accessibility statement

All data generated or analyzed during this study are included in this article. The datasets used and/or analyzed during the current study are available from the corresponding author on reasonable request.

Funding

Yunnan Fundamental Research Projects (Grant No. 202201AT070014), Open Project of the Clinical Medical Center of the First People's Hospital of Yunnan Province (Grant No. 2021LCZXXF-SJ04 , 2022LCZXKF-SJ03).

Authors' contributions

Guarantor of integrity of the entire study: Shuaifeng Yang, Xuehua Li.

Study concepts: Shuaifeng Yang.
Study design: Shuaifeng Yang.
Definition of intellectual content: Xuehua Li.
Literature research: Lide Jin.
Clinical studies: Weihua Tao.
Experimental studies: Guibo Zhang, Chengyuan Liu.
Data acquisition: Weihua Tao.
Data analysis: Xuehua Li.
Statistical analysis: Xuehua Li.
Manuscript preparation: Guibo Zhang.
Manuscript editing: Shuaifeng Yang.
Manuscript review: Shuaifeng Yang, Xuehua Li.

All authors have read and approved the final version of this manuscript to be published.

Declaration of competing interest

The authors declare that they have no known competing financial interests or personal relationships that could have appeared to influence the work reported in this paper.

Data availability

Data will be made available on request.

Acknowledgements

We thank everyone, who supports us to finish this study.

Appendix A. Supplementary data

Supplementary data to this article can be found online at https://doi.org/10.1016/j.redox.2023.102863.

References

[1] J. van Gijn, R.S. Kerr, G.J. Rinkel, Subarachnoid haemorrhage, Lancet 369 (9558) (2007) 306–318.
[2] M. Fujii, et al., Early brain injury, an evolving frontier in subarachnoid hemorrhage research, Transl Stroke Res 4 (4) (2013) 432–446.
[3] C. Rouanet, G.S. Silva, Aneurysmal subarachnoid hemorrhage: current concepts and updates, Arq Neuropsiquiatr 77 (11) (2019) 806–814.
[4] J. Chen, G.K.C. Wong, Microglia accumulation and activation after subarachnoid hemorrhage, Neural Regen Res 16 (8) (2021) 1531–1532.
[5] J. Chen, et al., Microglia activation, classification and microglia-mediated neuroinflammatory modulators in subarachnoid hemorrhage, Neural Regen Res 17 (7) (2022) 1404–1411.
[6] S. Yang, et al., Lipopolysaccharide preconditioning induces neuroprotection against early brain injury after experimental subarachnoid hemorrhage, Turk Neurosurg 24 (6) (2014) 839–843.
[7] T.H. Wang, et al., LPS pretreatment provides neuroprotective roles in rats with subarachnoid hemorrhage by downregulating MMP9 and Caspase3 associated with TLR4 signaling activation, Mol. Neurobiol. 54 (10) (2017) 7746–7760.
[8] R. Heinz, et al., Microglia as target for anti-inflammatory approaches to prevent secondary brain injury after subarachnoid hemorrhage (SAH), J. Neuroinflammation 18 (1) (2021) 36.
[9] D. Komander, M. Rape, The ubiquitin code, Annu. Rev. Biochem. 81 (2012) 203–229.
[10] K. Kliza, K. Husnjak, Resolving the complexity of ubiquitin networks, Front. Mol. Biosci. 7 (2020) 21.
[11] D. Komander, M.J. Clague, S. Urbe, Breaking the chains: structure and function of the deubiquitinases, Nat. Rev. Mol. Cell Biol. 10 (8) (2009) 550–563.
[12] J.G. Lee, et al., Characterization of the deubiquitinating activity of USP19 and its role in endoplasmic reticulum-associated degradation, J. Biol. Chem. 289 (6) (2014) 3510–3517.
[13] M. Wu, et al., USP19 deubiquitinates HDAC1/2 to regulate DNA damage repair and control chromosomal stability, Oncotarget 8 (2) (2017) 2197–2208.
[14] C.Q. Lei, et al., USP19 inhibits TNF-alpha- and IL-1 beta-triggered NF-kappaB activation by deubiquitinating TAK1, J. Immunol. 203 (1) (2019) 259–268.
[15] X. Wu, et al., Regulation of TRIF-mediated innate immune response by K27-linked polyubiquitination and deubiquitination, Nat. Commun. 10 (1) (2019) 4115.
[16] T. Liu, et al., USP19 suppresses inflammation and promotes M2-like macrophage polarization by manipulating NLRP3 function via autophagy, Cell. Mol. Immunol. 18 (10) (2021) 2431–2442.
[17] Y.Q. Xing, et al., The regulation of FOXO1 and its role in disease progression, Life Sci. 193 (2018) 124–131.
[18] H. Hao, et al., Protective mechanism of FoxO1 against early brain injury after subarachnoid hemorrhage by regulating autophagy, Brain Behav 11 (11) (2021) e2376.
[19] F. He, et al., Lowdose lipopolysaccharide inhibits neuronal apoptosis induced by cerebral ischemia/reperfusion injury via the PI3K/Akt/FoxO1 signaling pathway in rats, Mol. Med. Rep. 19 (3) (2019) 1443–1452.
[20] T. Mizuno, et al., Production of interleukin-10 by mouse glial cells in culture, Biochem. Biophys. Res. Commun. 205 (3) (1994) 1907–1915.
[21] K. Williams, et al., IL-10 production by adult human derived microglial cells, Neurochem. Int. 29 (1) (1996) 55–64.
[22] B. Laffer, et al., Loss of IL-10 promotes differentiation of microglia to a M1 phenotype, Front. Cell. Neurosci. 13 (2019) 430.
[23] I.D. Kyriazis, et al., KLF5 is induced by FOXO1 and causes oxidative stress and diabetic cardiomyopathy, Circ. Res. 128 (3) (2021) 335–357.
[24] T. Altay, et al., A novel method for subarachnoid hemorrhage to induce vasospasm in mice, J. Neurosci. Methods 183 (2) (2009) 136–140.
[25] X.P. Huang, et al., Peli 1 contributions in microglial activation, neuroinflammatory responses and neurological deficits following experimental subarachnoid hemorrhage, Front. Mol. Neurosci. 10 (2017) 398.
[26] J.H. Garcia, et al., Neurological deficit and extent of neuronal necrosis attributable to middle cerebral artery occlusion in rats. Statistical validation, Stroke 26 (4) (1995) 627–634, discussion 635.
[27] T. Sugawara, et al., A new grading system evaluating bleeding scale in filament perforation subarachnoid hemorrhage rat model, J. Neurosci. Methods 167 (2) (2008) 327–334.
[28] Y. Tian, et al., Activation of RARalpha receptor attenuates neuroinflammation after SAH via promoting M1-to-M2 phenotypic polarization of microglia and regulating Mafb/Msr1/PI3K-Akt/NF-kappaB pathway, Front. Immunol. 13 (2022), 839796.
[29] G.K. Wong, et al., Evaluation of cognitive impairment by the Montreal cognitive assessment in patients with aneurysmal subarachnoid haemorrhage: prevalence, risk factors and correlations with 3 month outcomes, J. Neurol. Neurosurg. Psychiatry 83 (11) (2012) 1112–1117.
[30] F.A. Sehba, et al., The importance of early brain injury after subarachnoid hemorrhage, Prog. Neurobiol. 97 (1) (2012) 14–37.
[31] R.M. Ransohoff, A polarizing question: do M1 and M2 microglia exist? Nat. Neurosci. 19 (8) (2016) 987–991.
[32] Z.V. Zheng, et al., The dynamics of microglial polarization reveal the resident neuroinflammatory responses after subarachnoid hemorrhage, Transl Stroke Res 11 (3) (2020) 433–449.
[33] S. Chung, et al., Distinct role of FoxO1 in M-CSF- and GM-CSF-differentiated macrophages contributes LPS-mediated IL-10: implication in hyperglycemia, J. Leukoc. Biol. 97 (2) (2015) 327–339.
[34] P. Hsu, et al., IL-10 potentiates differentiation of human induced regulatory T cells via STAT3 and Foxo1, J. Immunol. 195 (8) (2015) 3665–3674.
[35] J.M. Garcia, et al., Role of interleukin-10 in acute brain injuries, Front. Neurol. 8 (2017) 244.
[36] R.E. Ayer, J.H. Zhang, Oxidative stress in subarachnoid haemorrhage: significance in acute brain injury and vasospasm, Acta Neurochir. Suppl. 104 (2008) 33–41.
[37] F. Lin, et al., An update on antioxidative stress therapy research for early brain injury after subarachnoid hemorrhage, Front. Aging Neurosci. 13 (2021), 772036.
[38] D.Y. Xia, et al., SIRT1 promotes M2 microglia polarization via reducing ROS-mediated NLRP3 inflammasome signaling after subarachnoid hemorrhage, Front. Immunol. 12 (2021), 770744.